Functional Nanomaterials

DOI: 10.1002/anie.200906689

Au@MnO Nanoflowers: Hybrid Nanocomposites for Selective Dual Functionalization and Imaging**

*Thomas D. Schladt, Mohammed Ibrahim Shukoor, Kerstin Schneider, Muhammad Nawaz Tahir, Filipe Natalio, Irene Ament, Jan Becker, Florian D. Jochum, Stefan Weber, Oskar Köhler, Patrick Theato, Laura Maria Schreiber, Carsten Sönnichsen, Heinz C. Schröder, Werner E. G. Müller, and Wolfgang Tremel**

Dedicated to Professor Rüdiger Kniep on the occasion of his 65th birthday

Recently, the development of hybrid nanostructures consisting of various materials has attracted considerable interest. The assembly of different nanomaterials with specific optical, magnetic, or electronic properties to multicomponent composites can change and even enhance the properties of the individual constituents.[1] Specifically tuning the structure and interface interactions within the nanocomposites has resulted in novel platforms of materials that may lead the way to various future technologies, such as synchronous biolabeling, protein separation and detection,[2] heterogeneous catalysis,[3] and multimodal imaging in biomedicine.[4]

Of the various kinds of nanomaterials, gold nanorods show an unusually high polarizability at optical frequencies arising from the excitation of localized surface-plasmon resonances (LSPRs).[5,6] Furthermore, gold nanorods have promising therapeutic properties as hyperthermal agents because the local temperature around the gold nanorods can be increased by laser illumination through the tunable surface plasmon bands in the near infrared (NIR) region.[7] Using NIR radiation for hyperthermal therapy is beneficial because of the low absorption and low scattering by blood and tissue in this spectral range.[8]

Magnetic nanoparticles constitute another major class of nanomaterials that have attracted much research effort over the past decades.[9] In particular, exchange-coupled magnetic nanocomposites, such as antiferromagnetic/ferromagnetic core–shell nanoparticles, such as MnO/Mn_3O_4, have magnetic properties that are quite different from those of the individual components.[10] Concerning biomedical applications, superparamagnetic nanoparticles are attractive as contrast agents for magnetic resonance imaging (MRI). The majority of nanoparticles that have been investigated in this field comprise iron oxides (Fe_3O_4, γ-Fe_2O_3), which are known to shorten the transverse (or spin–spin) relaxation time T_2.[11] Recently, manganese oxide nanoparticles (MnO NPs) have been shown to be interesting candidates as contrast agents for shortening of the longitudinal (or spin-lattice) relaxation time T_1.[12] Consequently, a nanoparticulate system containing both an optically active plasmonic gold unit and a magnetically active MnO component would be advantageous for simultaneous optical and MRI detection.

Although considerable research efforts have been put into the chemical design of suitable surface ligands,[13] one of the major obstacles for biocompatible applications remains the lack of surface addressability. Therefore, a nanocomposite made up of individually addressable Au and MnO domains offers two functional surfaces for the attachment of different kinds of molecules, thus increasing both diagnostic and therapeutic potential.[14] Furthermore, the size of either of the two components can be varied to optimize the magnetic and optical properties. Herein we present the successful synthesis of Au@MnO nanocomposites consisting of both paramagnetic MnO NPs and Au crystallites followed by separate surface functionalization of both domains with fluorescent ligands.

Scheme 1 depicts a functionalized Au@MnO nanoflower with selective attachment of catechol anchors to the metal oxide petals and thiol anchors to the gold core. The nanoflowers were synthesized by decomposition of manganese acetylacetonate [$Mn(acac)_2$] in diphenyl ether in the presence of preformed Au NPs ("seeds"), with oleic acid and oleylamine as surfactants, following a similar procedure for the preparation of $Au@Fe_3O_4$ heteroparticles by Sun et al.[15] The

[*] T. D. Schladt, Dr. M. I. Shukoor, K. Schneider, Dr. M. N. Tahir, O. Köhler, Prof. Dr. W. Tremel
Institut für Anorganische Chemie und Analytische Chemie
Johannes-Gutenberg-Universität
Duesbergweg 10–14, 55099 Mainz (Germany)
Fax: (+49) 6131-39-25605
E-mail: tremel@uni-mainz.de

F. Natalio, Prof. Dr. Dr. H. C. Schröder, Prof. Dr. W. E. G. Müller
Institut für Physiologische Chemie
Universität Mainz (Germany)

I. Ament, J. Becker, Prof. Dr. C. Sönnichsen
Institut für Physikalische Chemie
Universität Mainz (Germany)

F. D. Jochum, Dr. P. Theato
Institut für Organische Chemie
Universität Mainz (Germany)

S. Weber, Prof. Dr. L. M. Schreiber
Institut für Medizinische Physik, Klinik und Polyklinik für Diagnostische und Interventionelle Radiologie
Universitätsklinikum Mainz (Germany)

[**] We are grateful to the Center for Complex Matter (COMATT) at the University of Mainz and POLYMAT, the state graduate school of excellence of Rhineland-Palatinate, and the Carl-Zeiss-Foundation for support.

Supporting information for this article is available on the WWW under http://dx.doi.org/10.1002/anie.200906689.

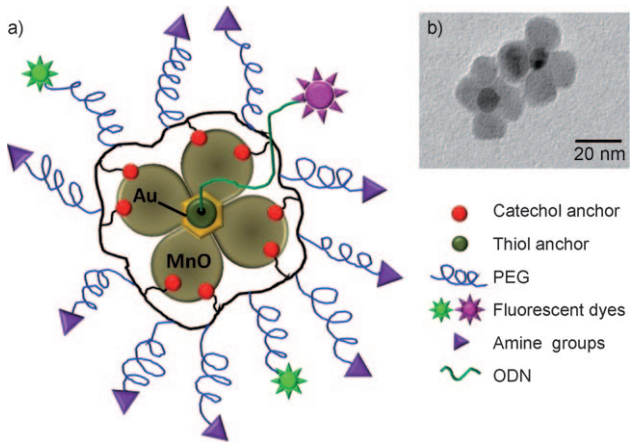

Scheme 1. a) Au@MnO nanoflowers separately functionalized using a multifunctional polymeric ligand carrying catechol anchor groups and a fluorescent dye (NBD) tagged to $PEG_{(800)}$ side groups. The gold core is functionalized with a Texas-Red-tagged thiolated oligonucleotide. b) TEM image of polymer-coated Au@MnO nanoflowers.

gold "seeds" were generated in situ by decomposition of gold acetate [$Au(OAc)_3$] at low temperature, which could be traced by a color change to deep red. At higher temperatures, MnO petals form by epitaxial growth on the surface of the Au NPs. The size and morphology of the nanoflowers can be varied by changing the molar ratio of the precursors (Figure 1). The number and size of the MnO petals increases with increasing [$Mn(acac)_2$]/[$Au(OAc)_3$] ratio. Furthermore, the variation in size and morphology is accompanied by a change in the optical and magnetic properties.

Figure 1 shows Au@MnO nanoflowers prepared with different precursor ratios. Increasing amount of mangenese precursor leads to larger MnO petals (see Supporting Information). In all cases the MnO particles nucleate heterogeneously on the gold seeds, and no unattached MnO NPs were observed. Phase purity was confirmed by powder X-ray diffraction (Supporting Information, Figure S1).

The magnetic properties of the nanocomposites were investigated to evaluate the influence of the diamagnetic Au cores on the MnO domains. Figure 2a shows magnetic hysteresis loops recorded at 5 K of Au@MnO nanoflowers with Au cores of 7 nm and MnO petals of approximately 10 nm and 18 nm, respectively. The nanocomposites are superparamagnetic; however, the saturation magnetization increases with MnO particle size, whereas the coercivity decreases. A more dramatic change can be seen in the field-cooled–zero-field-cooled (FC–ZFC) curves (Supporting Information, Figure S2), in which the magnetic blocking temperature increases to 35 K compared to pure MnO NPs.[16] A change in the magnetic behavior of the Au@Fe_3O_4 dumbbells depending on the size of the Fe_3O_4 domain was also reported by Sun et al.; the authors explained this behavior with thermal agitation of the nanoparticles and canting of the surface spins.[15]

The interaction of MnO and Au NPs leads to a red-shift of the gold plasmon resonance (Figure 2b). Pure Au NPs in the size range of 5–20 nm have a characteristic collective oscillation frequency (the plasmon resonance) at 520–525 nm,[17] the exact position varying with particle morphology and particle surface coating.[18] Attachment of the Au crystallites to MnO NPs leads to a significant shift of the extinction maximum to 555/585 nm (in the case of 7@10 nm and 7@18 nm Au@MnO particles, respectively). The red-shift is due to the MnO petals, which increase the effective local dielectric function around the gold cores; this effect may be evaluated quantitatively using the classical Mie theory[16,19–21] using literature values for the optical constants for Au NPs[22] and by approximating the local dielectric environment around these particles as a linear combination of the dielectric functions of the toluene solvent and the MnO.[23] Both experimental results confirm the assumption that the Au@MnO nanoflowers are both magnetically and optically active making them ideal candidates for multimodal biomedical imaging.

In the further course of our experiments, we investigated the addressability of both individual surfaces. First, the surfactant molecules on the MnO surface were replaced by a multidentate copolymer carrying catechol anchor groups and poly(ethylene glycol) linkers (PEG; $M_r \approx 800$) with free

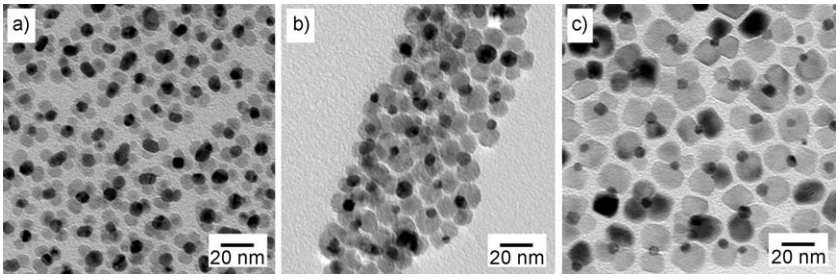

Figure 1. Au@MnO nanoflowers synthesized with different [$Mn(acac)_2$]/[$Au(OAc)_3$] molar ratios: a) 5:1, b) 10:1, and c) 20:1.

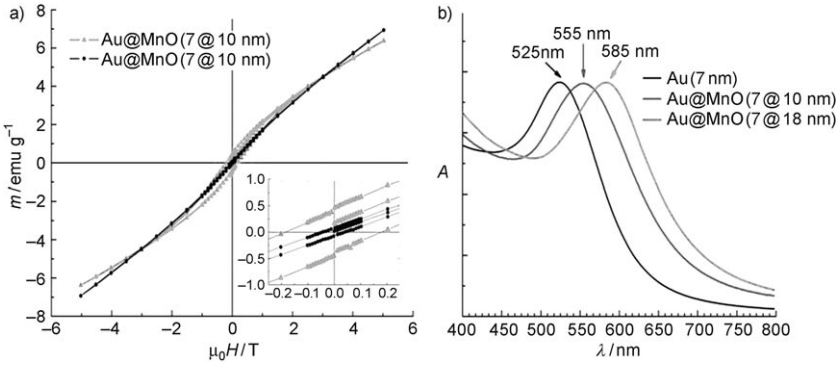

Figure 2. a) Magnetic hysteresis loops recorded at 5 K for Au@MnO nanoflowers with different petal sizes. b) UV/Vis spectra of Au NPs and of Au@MnO NPs of different sizes.

amino groups for further surface conjugation (Scheme 1).[24] To visualize the polymer functionalization, the fluorescent dye 4-chloro-7-nitrobenzofurazan (NBD) was conjugated to the amine groups of the polymer (Supporting Information, Figure S3).

Selective functionalization of the gold domain was achieved by incubating an aqueous solution of NBD-polymer-modified Au@MnO NPs with thiol-modified 24-mers customized oligonucleotide tagged with Texas red.[25] Excess reagents were removed by centrifugation. The functionalization approach is shown in Scheme 2. The polymer-functionalized Au@MnO NPs were stable against aggregation and precipitation in various aqueous media, including deionized water and PBS buffer solution for several days. Viability assays of nanocomposite solutions with the renal cell carcinoma line Caki-1 showed negligible toxicity of the nanoparticles even for concentrations as high as 140 $\mu g\,mL^{-1}$ (Supporting Information, Figure S6).

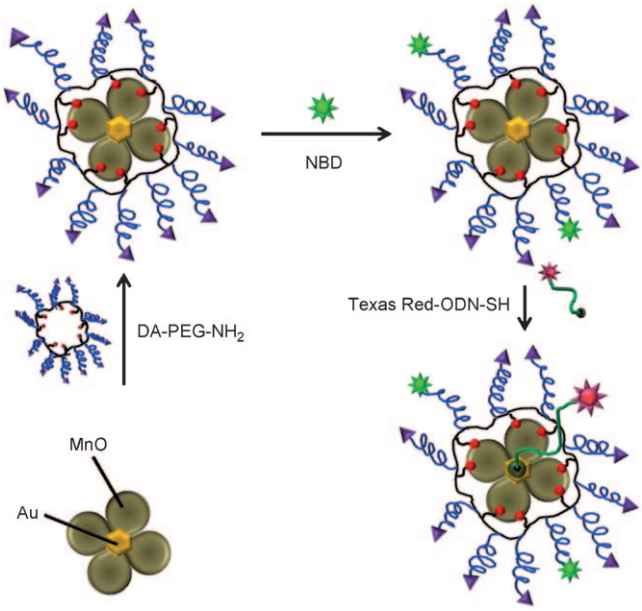

Scheme 2. Surface functionalization of Au@MnO nanoflowers with a multidentate copolymer and subsequent conjugation with NBD. The gold domain was selectively functionalized with a Texas-Red-tagged thiolated oligonucleotide. See Scheme 1 for definitions.

The nanoparticles were analyzed under an epifluorescent microscope at different emission wavelengths to visualize polymer-functionalized MnO domains (green fluorescence) and Texas-Red-tagged Au domains (red fluorescence). The co-localization of the green/red fluorescence signals in Figure 3a–c supports the idea that the nanoflowers are not only efficient as cargo-specific carriers but can simultaneously be used as optical probes for multimodal targeted delivery and imaging.

The optical properties of Au@MnO NPs were further explored with an optical transmission microscope in dark-field mode using a high-numerical aperture condenser and a 40× air objective.[26] The particles were immobilized in a flat glass capillary with hexane as embedding medium (Figure 3d,

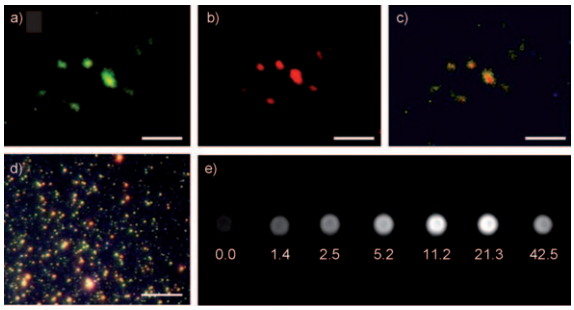

Figure 3. a) Fluorescence microscope images of NBD–polymer-functionalized 7@18 nm Au@MnO nanoflowers (green fluorescence), b) conjugated with Texas-Red-tagged thiolated oligonucleotide (red fluorescence), and c) a co-localized image. d) Real color picture of immobilized Au@MnO nanoflowers under dark-field illumination (all scale bars: 10 μm). e) T_1-weighted MRI images of aqueous solutions containing 7@18 nm Au@MnO nanoflowers (concentrations in mM Mn).

seen as separated bright colored spots, each corresponding to one single nanoparticle). Most of the spots appear green–yellow to the eye, with minor variances in color and intensity demonstrating a relatively low polydispersity. A few brighter red spots indicate a negligible number of aggregated particles with direct contact of the gold cores.

Investigation of a few dozen single particles shows a mean resonance wavelength $\lambda_{res} = 584 \pm 9$ nm and a mean spectral linewidth $\Gamma = 302 \pm 51$ meV (Supporting Information, Figure S4). These data agree well with the ensemble extinction spectrum of the sample (Figure 2b). Pure gold spheres of comparable size to the gold core (ca. 10 nm) would be hardly detectable with this experimental setup; therefore, surrounding MnO panels enlarge the total particle volume and significantly increase the amplitude of the scattered light. Calculations within the quasi-static approximation[27] show an increase of the scattering cross-sections for a 10 nm MnO layer ($n = 2.16$) by a factor of 23 together with a red-shift of the resonance of 76 nm (Supporting Information, Figure S5).

For magnetic resonance imaging, T_1 relaxivity measurements were performed on a clinical 3.0 Tesla scanner (Magnetom Trio, Siemens Medical Solutions, Erlangen, Germany) by means of a T_1 measurement using a centric reordered saturation recovery (SR) prepared snapshot fast low angle shot (SR-TurboFLASH) pulse sequence with different preparation times (T_I) ranging from 20 ms up to 8000 ms (other pulse sequence parameters: repetition time $T_R = 3.4$ ms, echo time $T_E = 1.5$ ms, flip angle = 20°). Figure 3e shows a T_1-weighted MR image of seven different MnO@Au nanocomposite concentrations dissolved in water ranging from 0 to 42.5 mM. T_1 measurement revealed a T_1 relaxivity of 0.224 $mM^{-1}ms^{-1}$ for the Au@MnO nanocomposites.

In summary, we have described the synthesis and characterization of a group of flowerlike Au@MnO NPs. By taking advantage of their constituent properties, different functional molecules were loaded onto each component of the heterostructure. The nanoparticles are magnetically and optically active, and they are therefore useful for simultaneous magnetic and optical detection. The fact that the nanoflowers are capable of imaging the same tissue area with both MRI

and an optical source without the fast signal loss observed in the common fluorescent labeling implies that they can be used to achieve high sensitivity in diagnostic imaging applications. It would be interesting to extend this synthetic method to nanoflowers made of different materials, such as Cu@MnO, Ag@MnO, or Pt@MnO, and to use these multidomain particles as building blocks of higher-order structures, the symmetries of which would derive from "directional" interactions between NP petals (for example, linear particle chains from nanoflowers having two leaves). Work on attaching therapeutic molecules to these dumbbell nanoparticles for target-specific imaging and delivery is currently underway.

Received: November 26, 2009
Published online: April 20, 2010

Keywords: magnetic properties · magnetic resonance imaging · manganese oxide · nanoparticles · surface functionalization

[1] a) M. A. Hines, P. Guyotsionnest, *J. Phys. Chem.* **1996**, *100*, 468 – 471; b) X. G. Peng, M. C. Schlamp, A. V. Kadavanich, A. P. Alivisatos, *J. Am. Chem. Soc.* **1997**, *119*, 7019 – 7029; c) Y.-W. Cao, U. Banin, *Angew. Chem.* **1999**, *111*, 3913 – 3916; *Angew. Chem. Int. Ed.* **1999**, *38*, 3692 – 3694; d) P. D. Cozzoli, T. Pellegrino, L. Manna, *Chem. Soc. Rev.* **2006**, *35*, 1195 – 1208; e) M. Hu, J. Chen, Z.-Y. Li, L. Au, G. V. Hartland, X. Li, M. Marquez, Y. Xia, *Chem. Soc. Rev.* **2006**, *35*, 1084 – 1094; f) H. Zeng, S. Sun, *Adv. Funct. Mater.* **2008**, *18*, 391 – 400; g) J. A. McGuire, J. Joo, J. M. Pietryga, R. Schaller, V. I. Klimov, *Acc. Chem. Res.* **2008**, *41*, 1810 – 1819; h) J. Gao, H. Gu, B. Xu, *Acc. Chem. Res.* **2009**, *42*, 1097 – 1107; i) C. Wang, H. Daimon, S. Sun, *Nano Lett.* **2009**, *9*, 1493 – 1496; j) C. Wang, J. Irudayaraj, *Small* **2010**, *6*, 283 – 289; k) S.-H. Choi, H. B. Na, Y. I. Park, K. An, S. G. Kwon, Y. Jang, M.-H. Park, J. Moon, J. S. Son, I. C. Song, W. K. Moon, T. Hyeon, *J. Am. Chem. Soc.* **2008**, *130*, 15573 – 15580.

[2] a) H. Gu, K. Xu, C. Xu, B. Xu, *Chem. Commun.* **2006**, 941 – 949; b) H. C. Schröder, F. Natalio, M. I. Shukoor, M. N. Tahir, W. Tremel, S. I. Belikov, A. Krasko, W. E. G. Müller, *Mol. Immunol.* **2008**, *45*, 945 – 953; c) M. I. Shukoor, F. Natalio, A. Krasko, H. C. Schröder, W. E. G. Müller, W. Tremel, *Chem. Commun.* **2007**, 4677 – 4679.

[3] a) S. Yang, Z. Peng, H. Yang, *Adv. Funct. Mater.* **2008**, *18*, 2745 – 2753; b) Q. Liu, Z. Yan, N. L. Henderson, J. C. Bauer, D. W. Goodman, J. D. Batteas, R. E. Schaak, *J. Am. Chem. Soc.* **2009**, *131*, 5720 – 5721; c) B. Lim, M. Jiang, P. H. C. Camargo, E. C. Cho, J. Tao, X. Lu, Y. Zhu, Y. Xia, *Science* **2009**, *324*, 1302 – 1305.

[4] a) J. Kim, S. Park, J. E. Lee, S. M. Jin, J. H. Lee, I. S. Lee, I. Yang, J. S. Kim, S. K. Kim, M. H. Cho, T. Hyeon, *Angew. Chem.* **2006**, *118*, 7918 – 7922; *Angew. Chem. Int. Ed.* **2006**, *45*, 7754 – 7758; b) C. J. Xu, J. Xie, D. Ho, C. Wang, N. Kohler, E. G. Walsh, J. R. Morgan, Y. E. Chin, S. H. Sun, *Angew. Chem.* **2008**, *120*, 179 – 182; *Angew. Chem. Int. Ed.* **2008**, *47*, 173 – 176; c) M. Liong, J. Lu, M. Kovochich, T. Xia, S. G. Ruehum, A. E. Nel, F. Tamanoi, J. I. Zink, *ACS Nano* **2008**, *2*, 889 – 896; d) L. Y. Wang, J. W. Bai, Y. J. Li, Y. Huang, *Angew. Chem.* **2008**, *120*, 2473 – 2476; *Angew. Chem. Int. Ed.* **2008**, *47*, 2439 – 2442; e) H. Park, J. Yang, S. Seo, K. Kim, J. Suh, D. Kim, S. Haam, K. H. Yoo, *Small* **2008**, *4*, 192 – 196; f) C.-K. Kim, P. Ghosh, V. M. Rotello, *Nanoscale*, **2009**, 1, 61 – 67.

[5] J. Becker, I. Zins, A. Jakab, Y. Khalavka, O. Schubert, C. Sönnichsen, *Nano Lett.* **2008**, *8*, 1719 – 1723.

[6] J. Pérez-Juste, I. Pastoriza-Santos, L. M. Liz-Marzán, P. Mulvaney, *Coord. Chem. Rev.* **2005**, *249*, 1870 – 1901.

[7] a) X. H. Huang, I. H. El-Sayed, W. Qian, M. A. El-Sayed, *J. Am. Chem. Soc.* **2006**, *128*, 2115 – 2120; b) R. S. Norman, J. W. Stone, A. Gole, C. J. Murphy, T. L. Sabo-Attwood, *Nano Lett.* **2008**, *8*, 302 – 306; c) E. B. Dickerson, E. C. Dreaden, X. Huang, I. H. El-Sayed, H. Chu, S. Pushpanketh, J. F. McDonald, M. A. El-Sayed, *Cancer Lett.* **2008**, *269*, 57 – 66.

[8] a) R. Weissleder, C.-H. Tung, U. Mahmood, A. Bogdanov, Jr., *Nat. Biotechnol.* **1999**, *17*, 375 – 378; b) A. Becker, C. Hessenius, K. Licha, B. Ebert, U. Sukowski, W. Semmler, B. Wiedenmann, C. Grötzinger, *Nat. Biotechnol.* **2001**, *19*, 327 – 331.

[9] a) V. Salgueiriño-Maceira, M. A. Correa-Duarte, M. Farle, *Small* **2005**, *1*, 1073 – 1076; b) C. H. Jun, Y. J. Park, Y. R. Yeon, J. R. Choi, W. R. Lee, S. J. Ko, J. Cheon, *Chem. Commun.* **2006**, 1619 – 1621; c) S. S. Kang, G. X. Miao, S. Shi, Z. Jia, D. E. Nikles, J. W. Harrell, *J. Am. Chem. Soc.* **2006**, *128*, 1042 – 1043; d) Y. W. Jun, J.-W. Seo, J. W. Cheon, *Acc. Chem. Res.* **2008**, *41*, 179 – 189; e) M. I. Bodnarchuk, M. V. Kovalenko, H. Groiss, R. Resel, M. Reissner, G. Hesser, R. T. Lechner, W. Steiner, F. Schäffler, W. Heiss, *Small* **2009**, *5*, 2247 – 2252.

[10] a) H. Zeng, J. Li, J. P. Liu, Z. L. Wang, S. Sun, *Nature* **2002**, *420*, 395 – 398; b) H. Zeng, J. Li, Z. L. Wang, J. P. Liu, S. Sun, *Nano Lett.* **2004**, *4*, 187 – 190; c) A. E. Berkowitz, G. F. Rodriguez, J. I. Hong, K. An, T. Hyeon, N. Agarwal, D. J. Smith, E. E. Fullerton, *Phys. Rev. B* **2008**, *77*, 024403; d) X. Peng, C. Schlamp, A. V. Kadavanich, A. P. Alivisatos, *J. Am. Chem. Soc.* **1997**, *119*, 7019 – 7029; e) M. A. Malik, P. O'Brien, N. Revaprasadu, *Chem. Mater.* **2002**, *14*, 2004 – 2010; f) S. Decker, K. J. Klabunde, *J. Am. Chem. Soc.* **1996**, *118*, 12465 – 12466.

[11] a) S. Mansson, A. Bjornerud in *The Chemistry of Contrast Agents in Medical Magnetic Resonance Imaging* (Eds.: A. E. Merbach, E. Toth), Wiley, New York, **2001**, pp. 1 – 44; b) Y. W. Jun, J. H. Lee, J. W. Cheon, *Angew. Chem.* **2008**, *120*, 5200 – 5213; *Angew. Chem. Int. Ed.* **2008**, *47*, 5122 – 5135.

[12] H. B. Na, J. H. Lee, K. An, Y. I. Park, M. Park, I. S. Lee, D. H. Nam, S. T. Kim, S. H. Kim, S. W. Kim, K. H. Lim, K. S. Kim, S.-O. Kim, T. Hyeon, *Angew. Chem.* **2007**, *119*, 5493 – 5497; *Angew. Chem. Int. Ed.* **2007**, *46*, 5397 – 5401.

[13] a) M. I. Shukoor, F. Natalio, V. Ksenofontov, H. C. Schröder, W. E. G. Müller, W. Tremel, *Small* **2007**, *3*, 1374 – 1378; b) M. I. Shukoor, F. Natoli, N. Glube, M. N. Tahir, H. A. Therese, V. Ksenofontov, N. Metz, P. Theato, P. Langguth, J.-P. Boissel, H.-C. Schröder, W. E. G. Müller, W. Tremel, *Angew. Chem.* **2008**, *120*, 4826 – 4830; *Angew. Chem. Int. Ed.* **2008**, *47*, 4748 – 4752; c) M. I. Shukoor, F. Natalio, P. Gupta, M. N. Tahir, H. A. Therese, S. Weber, S. Fischer, N. Metz, P. Theato, L. M. Schreiber, H. C. Schröder, W. E. G. Müller, W. Tremel, *Adv. Funct. Mater.* **2009**, *19*, 3717 – 3725.

[14] C. Xu, J. Xie, D. Ho, C. Wang, N. Kohler, E. G. Walsh, J. R. Morgan, Y. E. Chin, S. H. Sun, *Angew. Chem.* **2008**, *120*, 179 – 182; *Angew. Chem. Int. Ed.* **2008**, *47*, 173 – 176.

[15] H. Yu, M. Chen, P. M. Rice, S. X. Wang, R. L. White, S. Sun, *Nano Lett.* **2005**, *5*, 379 – 382.

[16] a) W. S. Seo, H. H. Jo, K. Lee, B. Kim, S. J. Oh, J. T. Park, *Angew. Chem.* **2004**, *116*, 1135 – 1137; *Angew. Chem. Int. Ed.* **2004**, *43*, 1115 – 1117; b) T. D. Schladt, T. Graf, W. Tremel, *Chem. Mater.* **2009**, *21*, 3183 – 3190.

[17] a) M. Faraday, *Philos. Trans. R. Soc. London* **1857**, *147*, 1145 – 1181; b) U. Kreibig, M. Vollmer, *Optical Properties of Metal Clusters*, *Vol. 25*, Springer, Berlin, **1995** (Springer Series in Materials Science); c) G. Raschke, S. Kowarik, T. Franzl, C. Sönnichsen, T. A. Klar, J. Feldmann, A. Nichtl, K. Kürzinger, *Nano Lett.* **2003**, *3*, 935 – 938; d) K. Kelly, E. Coronado, L. L. Zhao, G. C. Schatz, *J. Phys. Chem. B* **2003**, *107*, 668 – 677; e) M.-C. Daniel, D. Astruc, *Chem. Rev.* **2004**, *104*, 293 – 346.

[18] a) B. Rothenhäusler, W. Knoll, *Opt. Commun.* **1987**, *63*, 301 – 304; b) G. Nelles, H. Schönherr, M. Jaschke, H. Wolf, M. Schaub,

J. Küther, W. Tremel, E. Bamberg, H. Ringsdorf, H.-J. Butt, *Langmuir* **1998**, *14*, 808 – 815.
[19] G. Mie, *Ann. Phys.* **1908**, *25*, 377 – 445.
[20] a) A. Pinchuk, U. Kreibig, *New J. Phys.* **2003**, *5*, 151.1 – 151.15; b) A. O. Pinchuk, A. M. Kalsin, B. Kowalczyk, G. C. Schatz, B. A. Grzybowski, *J. Phys. Chem. C* **2007**, *111*, 11816 – 11822; c) Y. Wei, R. Klajn, A. O. Pinchuk, B. A. Grzybowski, *Small* **2008**, *4*, 1635 – 1639.
[21] Z. Hens, D. Vanmaekelbergh, E. Stoffels, H. van Kempen, *Phys. Rev. Lett.* **2002**, *88*, 236803.
[22] P. B. Johnson, R. W. Christy, *Phys. Rev. B* **1972**, *6*, 4370 – 4379.
[23] K. J. Kim, Y. R. Park, *J. Cryst. Growth* **2004**, *270*, 162 – 167.
[24] a) M. Eberhardt, R. Mruk, P. Theato, R. Zentel, *Eur. Polym. J.* **2005**, *41*, 1569 – 1575; b) M. N. Tahir, M. Eberhardt, P. Theato, S. Faiß, A. Janshoff, T. Gorelik, U. Kolb, W. Tremel, *Angew. Chem.* **2006**, *118*, 922 – 926; *Angew. Chem. Int. Ed.* **2006**, *45*, 908 – 912.
[25] J. J. Storhoff, R. Elghanian, R. C. Mucic, C. A. Mirkin, R. L. Letsinger, *J. Am. Chem. Soc.* **1998**, *120*, 1959 – 1964.
[26] J. Becker, O. Schubert, C. Sönnichsen, *Nano Lett.* **2007**, *7*, 1664 – 1669.
[27] M. Liu, P. Guyot-Sionnest, *J. Phys. Chem. B* **2004**, *108*, 5882 – 5888.

